

Delays, Inaccuracies and Anticipation in Microscopic Traffic Models

Martin Treiber, Arne Kesting, Dirk Helbing

*Institute for Transport & Economics, Dresden University of Technology,
Andreas-Schubert-Strasse 23, D-01062 Dresden, Germany*

Abstract

We generalize a wide class of time-continuous microscopic traffic models to include essential aspects of traffic dynamics not captured by these models, but relevant for human drivers. Specifically, we consider (i) finite reaction times and limited attention, (ii) estimation errors, (iii) looking several vehicles ahead (spatial anticipation), (iv) temporal anticipation, and (v) long-term adaptation to the global traffic situation. The estimation errors are modelled as stochastic Wiener processes and lead to time-correlated fluctuations of the acceleration.

We have applied these generalizations to the intelligent-driver model and show that the destabilizing effects of reaction times, limited attention, and estimation errors can essentially be compensated for by spatial and temporal anticipation, that is, the combination of stabilizing and destabilizing effects result in the same qualitative macroscopic dynamics as that of the underlying simple car-following model which, in many cases, justifies the use of the latter. While the qualitative dynamics is unchanged, the effects of multi-anticipation increase both spatial and temporal scales of complex patterns of congested traffic such as stop-and-go waves and smear out the transition zones between free and congested traffic states, in agreement with real traffic data. Remarkably, the anticipation mechanisms allow accident-free smooth driving in complex traffic situations even if reaction times exceed typical time headways.

Key words: Transport processes, Phase transitions, Nonhomogeneous flows, Transportation

PACS: 05.60.-k, 05.70.Fh, 47.55.-t, 89.40

Email addresses: treiber@vwi.tu-dresden.de (Martin Treiber),
kesting@vwi.tu-dresden.de (Arne Kesting), helbing1@vwi.tu-dresden.de
(Dirk Helbing).

URLs: <http://www.mtreiber.de> (Martin Treiber), <http://www.akesting.de>
(Arne Kesting), <http://www.helbing.org> (Dirk Helbing).

1 Introduction

The nature of human driving behavior and the differences to automated driving implemented in most micromodels is a controversial topic in traffic science [1–4]. Finite reaction times, finite estimation capabilities and limited attention spans impair the human driving performance and stability compared to automated driving, sometimes called 'adaptive cruise control' (ACC). However, unlike machines, human drivers routinely scan the traffic situation several vehicles ahead and anticipate future traffic situations leading, in turn, to an increased stability.

The question arises how these antagonistic effects affect the overall driving behavior and performance, and whether, in typical situations, the stabilizing or the destabilizing effects dominate, or if they effectively cancel out each other. The answers to these questions are crucial in determining the influence of a growing number of vehicles equipped with automated acceleration control on the overall traffic flow. Up to now, there is not even clarity about the sign of the effect. Some investigations predict a positive effect [5] while others are more pessimistic [6].

Single aspects of human driving behavior have been investigated in the past. For example, it is well known that traffic instabilities increase with the reaction times T' of the drivers. Finite reaction times in time-continuous models are implemented by evaluating the right-hand side of the equation for the acceleration (or velocity) at some previous time $t - T'$ with $T' > 0$ [7–9]. A different approach consists in interpreting the update time interval Δt in time-discrete models such as cellular automata (CA) [10] directly as a reaction time. However, as is shown in Sec. 3.1.1 below, these two approaches are not necessarily equivalent. Reaction times in time-continuous models have been modelled as early as 1961 by Newell [7]. Recently, the optimal-velocity model (OVM) [11] has been extended to include finite reaction times [8]. However, the Newell model has no dynamic velocity, and the OVM with delay turns out to be accident-free only for unrealistically small reaction times [12].

To overcome this deficiency, Davis [9] introduced (among other modifications) an anticipation of the expected future gap to the front vehicle allowing accident-free driving at reaction times of 1 s. However, reaction times were not fully implemented in [9] since the own velocity, which is one of the stimuli on the right-hand side of the acceleration equation, has been taken at the actual rather than at the delayed time. Furthermore, in some traffic situations such as stop-and-go traffic, after active or passive lane changes, or when accelerating on an empty road, the OVM leads to unrealistically high accelerations of the order of $v_0/\tau = 30 \text{ m/s}^2$ for typical parameter values ($v_0 = 30 \text{ m/s}$ for the maximum velocity and $\tau = 1 \text{ s}$ for the velocity relaxation time).

Another approach to model temporal anticipations consists in including the acceleration of the preceding vehicles to the input variables of the model. For cellular automata, this has been implemented by introducing a binary-valued “brake light” variable [13].

To our knowledge, there exists no car-following model exhibiting platoon stability for reaction times (with respect to all stimuli) exceeding half of the time headway of the platoon vehicles. Human drivers, however, accomplish this easily. In dense (not yet congested) traffic, the most probable time headways on German freeways are 0.9-1s [14,15] which is of the same order as typical reaction times [16].

Moreover, single-vehicle data for German freeways [14,15] indicate that some drivers drive at headways as low as 0.3 s, which is below the reaction time of even a very attentive driver by a factor of at least 2-3 [16]. For principal reasons, therefore, safe driving is not possible in this case when considering only the immediate vehicle in front.

This suggests that human drivers achieve additional stability and safety by taking into account next-nearest neighbors and further vehicles ahead as well, which we will denote by ‘spatial anticipation’ or ‘multi-anticipation’ [17].

Spatial multi-anticipation in traffic models has been applied to the OVM [17] and to the Gipps model [18] as well as to some cellular automata model [13,19]. As expected, the resulting ‘multi-anticipative’ models show a higher stability than the original model. However, the stability of the aforementioned models is still smaller than that of human driving. Furthermore, they display unrealistic behavior such as clustering in pairs [18], or a too high backwards propagation velocities of perturbations in congested traffic ($v_g = -30$ km/h) [17].

Besides reacting to the immediate traffic environment, human drivers adapt their driving style on a longer time scale to the traffic situation [20] such that the actual driving style depends on the traffic conditions of the last few minutes (so-called ‘memory effect’ [21]). For example, most drivers increase the time headways to the leading vehicle after driving some time in congested traffic [20,22], which is sometimes termed ‘resignation effect’ [23,24].

Imperfect estimation capabilities often serve as motivation or justification to introduce stochastic terms into micromodels such as the Gipps model [25] (see also [1,26]). Most cellular automata require fluctuating terms as well. In nearly all the cases, fluctuations are assumed to be δ -correlated in time and acting directly on the accelerations. An important feature of human estimation errors, however, is a certain persistency. If one underestimates, say, the distance at time t , the probability of underestimating it at the next time step (which typically is less than 1 s in the future) is very high as well. Another source leading to temporally correlated acceleration noise is the tendency of human

drivers to actively adapt to the traffic situation, i.e., to change the acceleration, only at discrete times when the discrepancy with respect to the intrinsically intended driving style exceeds a certain threshold [27].

In this paper, we propose the human driver model (HDM) in terms of five extensions applicable to a wide class of basic car-following models. The HDM incorporates into these models (i) finite reaction times, (ii) estimation errors, (iii) spatial anticipation, (iv) temporal anticipation, and (v) adaptation to the global traffic situation. The class of suitable basic models is characterized by continuous acceleration functions depending on the velocity, the gap, and the velocity of the preceding car and includes, for example, the optimal-velocity model (OVM) [11], the Gipps model [28], the intelligent-driver model (IDM) [29], and the boundedly rational driver model [30,31].

For the matter of illustration we will apply the HDM extensions to the IDM, which has a built-in anticipative and smooth braking strategy and reaches good scores in a first independent attempt to benchmark micromodels based on real traffic data [32].

In Sec. 2, we will formulate the HDM in terms of extensions for the acceleration function of the basic model.

In Sec. 3 we will simulate the stability of vehicle platoons as a function of reaction time T' and number of anticipated vehicles n_a and find string stability for arbitrarily long platoons for reaction times of up to 1.5 s. We will show that both, spatial and temporal anticipation plays a crucial role. Furthermore, we simulate the macroscopic effects for an open system containing a flow-conserving bottleneck [33,29,34]. We find that multi-vehicle anticipation ($n_a > 1$) can compensate for the destabilizing effects of reaction times and estimation errors and determine a phase diagram for the corresponding parameter space. When simultaneously increasing T' and n_a such that the stability is maintained, we discover that the wavelength of stop-and-go waves increases and the fronts between free and congested traffic become smoother, in accordance with observations.

In the concluding Section 4 we suggest applications and further investigations and discuss some aspects of human driving that are not included in the HDM.

2 Modelling human driver behavior

In the following, we will formulate various aspects of human driving in a model-independent way in terms of generalizations to existing micromodels. Here, we will restrict ourselves to single-lane longitudinal dynamics. Specifically, we will

consider time-continuous micromodels (car-following models) of the general form

$$\frac{dv_\alpha}{dt} = a^{\text{mic}}(s_\alpha, v_\alpha, \Delta v_\alpha), \quad (1)$$

where the own velocity v_α , the net distance s_α , and the velocity difference Δv_α to the leading vehicle serve as stimuli determining the acceleration a^{mic} [35].

This class of basic models is characterized by (i) instantaneous reaction, (ii) reaction only to the immediate predecessor, (iii) infinitely exact estimating capabilities of drivers regarding the input stimuli s , v , and Δv , and (iv) an acceleration that is uniquely determined by the local traffic environment, i.e., there is no long-term adaptation to the global traffic situation [21]. In some sense, such models describe driving behavior similar to adaptive cruise control systems.

2.1 Finite reaction time

A reaction time T' is implemented simply by evaluating the right-hand side of Eq. (1) at time $t - T'$. If T' is not a multiple of the update time interval, we have used a linear interpolation according to

$$x(t - T') = \beta x_{t-n-1} + (1 - \beta)x_{t-n}, \quad (2)$$

where x denotes any quantity on the right-hand side of (1) such as s_α , v_α , or Δv_α , and x_{t-n} denotes this quantity taken $n = \text{floor}(T'/\Delta t)$ time steps before the actual step. The weight factor of the linear interpolation is given by $\beta = T'/\Delta t - n$. We emphasize that *all* input stimuli s_α , v_α , and Δv_α are evaluated at the delayed time.

Notice that the reaction time T' is sometimes set equal to the 'safety' time-headway T or to the update time interval Δt of the explicit numerical integration. It is, however, essential to distinguish between these times conceptually. Setting $T = T'$ corresponds to the lower limit of safe driving *only* if considering a worst-case scenario in which (i) the preceding vehicle suddenly brakes to a stop at maximum deceleration, (ii) the velocities of the leading and the following vehicle are the same, (iii) the maximum decelerations are the same, and (iv) no multi-anticipation is considered. In reality, T depends on the driving style and T' on physiological parameters which are, at most, weakly correlated. The difference between T' and Δt is further elaborated in Sec. 3.1.1.

2.2 Imperfect estimation capabilities

We will now model estimation errors for the net distance s and the velocity difference Δv to the preceding vehicle. Since the velocity itself can be obtained by looking at the speedometer, we neglect its estimation error. From empirical investigations (for an overview see [1], p. 190) it is known that the uncertainty of the estimation of Δv is proportional to the distance, i.e., one can estimate the inverse of the time-to collision (TTC) $|\Delta v|/s$ with a constant uncertainty [36]. For the distance itself, we specify the estimation error in a relative way, i.e., we assume a constant variation coefficient V_s of the errors. Furthermore, in contrast to other stochastic micromodels [10], we want to take into consideration that, obviously, estimation errors have a certain correlation time which can be modelled by a Wiener process [37]. This leads to the following nonlinear stochastic processes for the distance and the velocity difference,

$$s^{\text{est}}(t) = s(t) \exp(V_s w_s(t)), \quad (3)$$

and

$$(\Delta v)^{\text{est}}(t) = \Delta v + s(t) r_c w_{\Delta v}(t), \quad (4)$$

where $V_s = \sigma_s / \langle s \rangle$ with $\sigma_s^2 = \langle (s - \langle s \rangle)^2 \rangle$ is the variation coefficient of the distance estimate, and r_c the inverse TTC as measure of the error in Δv . The stochastic variables $w_s(t)$ and $w_{\Delta v}(t)$ obey independent Wiener processes $w(t)$ of variance 1 with correlation times $\tau = \tau_s$ and $\tau_{\Delta v}$, respectively, defined by [37]

$$\frac{dw}{dt} = -\frac{w}{\tau} + \xi(t), \quad (5)$$

with

$$\langle \xi \rangle = 0, \quad \langle \xi(t) \xi(t') \rangle = \frac{2}{\tau} \delta(t - t'). \quad (6)$$

In the explicit numerical update from time step t to step $t+1$, we implemented the Wiener processes by the approximations

$$w_{t+1} = e^{-\Delta t/\tau} w_t + \sqrt{\frac{2\Delta t}{\tau}} \eta_t, \quad (7)$$

where the $\{\eta_t\}$ are independent realizations of a Gaussian distributed quantity with zero mean and unit variance. We checked numerically that the update scheme (7) satisfies the fluctuation-dissipation theorem $\langle w_t^2 \rangle = 1$ for any update time interval satisfying $\Delta t \ll \tau$.

2.3 Temporal anticipation

We will assume that drivers are aware of their finite reaction time and anticipate the traffic situation accordingly. Besides anticipating the future distance [9], we will anticipate the future velocity using a constant-acceleration heuristics. The combined effects of a finite reaction time, estimation errors and temporal anticipation leads to the following input variables for the underlying micromodel (1),

$$\frac{dv}{dt} = a^{\text{mic}}(s'_\alpha, v'_\alpha, \Delta v'_\alpha), \quad (8)$$

with

$$s'_\alpha(t) = [s_\alpha^{\text{est}} - T' \Delta v_\alpha^{\text{est}}]_{t-T'}, \quad (9)$$

$$v'_\alpha(t) = [v_\alpha^{\text{est}} + T' a_\alpha]_{t-T'}, \quad (10)$$

and

$$\Delta v'_\alpha(t) = \Delta v_\alpha^{\text{est}}(t - T'). \quad (11)$$

We did not apply the constant-acceleration heuristics for anticipating the future velocity difference or the future distance, since the accelerations of other vehicles cannot be estimated reliably by human drivers. Instead, we applied the simpler constant-velocity heuristics for these cases.

Notice that the anticipation terms discussed in this subsection (which do not involve any additional model parameters) are specifically designed to compensate for the reaction time by means of plausible heuristics. They are to be distinguished from possible 'anticipative' terms of some models which are typically aiming at collision-free driving in a 'worst-case' scenario (sudden braking of the preceding vehicle to a standstill) at limited braking deceleration. Such terms typically depend on the velocity difference and are included, e.g., in the Gipps model, in the IDM, and in some cellular automata [19,38], but notably not in the OVM. The HDM is most effective when using a basic model with some sort of anticipation.

2.4 Spatial anticipation several vehicles ahead

Let us now split up the acceleration of the underlying microscopic model into a single-vehicle acceleration valid on a nearly empty road which depends only

on the considered vehicle α , and a two-vehicle braking deceleration taking into account the vehicle-vehicle interaction with the preceding vehicle,

$$a^{\text{mic}}(s_\alpha, v_\alpha, \Delta v_\alpha) := a_\alpha^{\text{free}} + a^{\text{int}}(s_\alpha, v_\alpha, \Delta v_\alpha). \quad (12)$$

Notice that this decomposition of the acceleration has already been used to formulate a lane-changing model for a wide class of micromodels [39].

Next, we model the reaction to several vehicles ahead just by summing up the corresponding vehicle-vehicle pair interactions $a_{\alpha\beta}^{\text{int}}$ from vehicle β to vehicle α for the n_a nearest preceding vehicles β :

$$\frac{d}{dt}v_\alpha(t) = a_\alpha^{\text{free}} + \sum_{\beta=\alpha-n_a}^{\alpha-1} a_{\alpha\beta}^{\text{int}}, \quad (13)$$

where all distances, velocities and velocity differences on the right-hand sides are given by (9) - (11). Each pair interaction from vehicle β to vehicle α is given by

$$a_{\alpha\beta}^{\text{int}} = a^{\text{int}}(s_{\alpha\beta}, v_\alpha, v_\alpha - v_\beta), \quad (14)$$

where

$$s_{\alpha\beta} = \sum_{j=\beta+1}^{\alpha} s_j \quad (15)$$

is the sum of all *net* gaps between the vehicles α and β

2.5 Adaptation of the driving style to the traffic environment

It is observed that most drivers increase their preferred temporal headway, after being stuck in congested traffic for some time [20,40]. Furthermore, when larger gaps appear or when reaching the downstream front of the congested zone, human drivers accelerate less and possibly decrease their desired velocity compared to a free-traffic situation.

We model this *memory effect* [21] by assuming that, when encountering congested traffic characterized by a low 'level-of service' $\lambda = v_\alpha/v_0$, drivers gradually adapt their driving style from a 'free-traffic mode' to a 'congested-traffic mode'. This typically involves a gradual change of some parameters of the underlying car-following model as a function of the new, slowly varying dynamical variable $\lambda(t)$. Specifically, for the IDM used in this work, we changed the IDM parameters a and T valid for free traffic according to $a(\lambda) = a[1 + (1 - \lambda)(\beta_a - 1)]$ and $T(\lambda) = T[1 + (1 - \lambda)(\beta_T - 1)]$, cf. Table 2. The adaptations take place on a time scale τ of the order of a few minutes. Further details are given in [21].

2.6 Applying the HDM on the IDM

In this paper, we will apply the HDM generalizations to the IDM. In this model [29], the acceleration of each vehicle α is assumed to be a continuous function of the velocity v_α , the net distance gap s_α , and the velocity difference (approaching rate) Δv_α to the leading vehicle:

$$\dot{v}_\alpha = a \left[1 - \left(\frac{v_\alpha}{v_0} \right)^4 - \left(\frac{s^*(v_\alpha, \Delta v_\alpha)}{s_\alpha} \right)^2 \right]. \quad (16)$$

This expression is an interpolation of the tendency to accelerate with $a_f(v) := a[1 - (v/v_0)^4]$ on a free road and the tendency to brake with deceleration $-b_{\text{int}}(s, v, \Delta v) := -a(s^*/s)^2$, when vehicle α comes too close to the vehicle in front. The deceleration term depends on the ratio between the effective 'desired minimum gap' s^* and the actual gap s_α , where the desired gap

$$s^*(v, \Delta v) = s_0 + vT + \frac{v\Delta v}{2\sqrt{ab}} \quad (17)$$

is dynamically varying with velocity. The minimum distance s_0 in jams is significant for low velocities only. The main contribution in stationary traffic is the term vT which corresponds to following the preceding vehicle with a constant 'safety' net time gap T . The last term is only active in non-stationary traffic and implements an accident-free 'intelligent' driving behavior including a braking strategy that, in nearly all situations, limits braking decelerations to the 'comfortable deceleration' b .

Renormalisation for the IDM

For the IDM, there exists a closed-form solution of the multi-anticipative equilibrium distance as a function of the velocity,

$$s_e(v) = \gamma s^*(v, 0) \left[1 - \left(\frac{v}{v_0} \right)^\delta \right]^{-\frac{1}{2}}, \quad (18)$$

which is γ times the equilibrium distance of the original IDM [29], where

$$\gamma = \sqrt{\sum_{\alpha=1}^{n_a} \frac{1}{\alpha^2}}. \quad (19)$$

Parameter	Value
Desired velocity $v_0 = v_{0,\max}$	128 km/h
Save time headway $T = T_{\min}$	1.1 s
Maximum acceleration a	1 m/s ²
Desired deceleration b	1.5 m/s ²
Jam distance s_0	2 m

Table 1

Model parameters of the IDM as used in this paper. The vehicle length is 5 m. In the string stability szenario, v_0 and T are adopted to the parameters used in [12].

Parameter	value
Reaction time T'	0 s - 1.6 s
Update time interval Δt	0.01 s - 2.5 s
Number of anticipated vehicles n_a	1 - 8
Relative distance error V_s	5%
Inverse TTC error r_c	0.01/s
error correlation times $\tau_s, \tau_{\Delta v}$	20 s
Traffic adaptation factor β_a	0.5
Traffic adaptation factor β_T	1.3
Traffic adaptation time τ	120 s

Table 2

Parameters of the human-driver extensions with the values used in this paper.

The equilibrium distance $s_e(v)$ can be transformed to that of the original IDM by renormalizing the relevant IDM parameters appearing in $s^*(v, 0)$:

$$s_0^{\text{ren}} = \frac{s_0}{\gamma}, \quad T^{\text{ren}} = \frac{T}{\gamma}. \quad (20)$$

The above renormalisation will be applied to all simulations of this paper.

Notice that in the limiting case of anticipation to arbitrary many vehicles we obtain $\lim_{n_a \rightarrow \infty} \gamma(n_a) = \pi/\sqrt{6} = 1.283$. This means that the combined effects of all non-nearest-neighbor interactions would lead to an increase of the equilibrium distance by just about 28%.

3 Simulations and results

In this section, we use the HDM in combination with the IDM. Unless stated otherwise, we will use the IDM and HDM parameters given in the Tables 1 and 2, respectively. In the simulations presented in this paper, we will discuss extensively the destabilizing effects of increasing reaction time T' and update time intervals Δt , and the stabilizing effects of a growing number n_a of anticipated vehicles.

A short discussion of the other HDM parameters is in order. The stochastic sources V_s and r_c characterize the degree of the estimation uncertainty of the drivers. In agreement with expectation, traffic becomes more unstable when increasing V_s and r_c . In contrast to most cellular automata, there is no qualitative change in the dynamics for the deterministic case $V_s = r_c = 0$.

While the effect of the correlation times τ_a and $\tau_{\Delta v}$ on the macroscopic dynamics is relatively weak, acceleration time series of simulated floating-cars became increasingly jagged for decreasing correlation times. Notice that the limits $\tau_a \rightarrow \infty$ or $\tau_{\Delta v} \rightarrow \infty$ correspond to 'frozen' error amplitudes and essentially correspond to simulating heterogeneous traffic.

The parameters β_a , β_T and τ pertain to the 'memory effect' [21]. The more the values of the traffic adaptation factors β_a and β_T differ from unity, the more pronounced is the long-term adaptation to the overall traffic situation. Specifically, decreasing β_a or increasing β_T leads to more pronounced hysteresis effects ('capacity drop') with respect to the transitions from free to congested traffic and *vice versa*, and to increased wavelengths in case of oscillatory congested traffic. Furthermore, particularly for adaptation times τ exceeding 1 min, the scattering of the fundamental diagram in the congested region becomes more pronounced.

Notice that all human-driver extensions are switched off (i.e., the original basic model is recovered) for the HDM values $T' = 0$, $V_s = 0$, $r_c = 0$, $n_a = 1$, and $\beta_a = \beta_T = 1$.

For all simulations, we have used an explicit integration scheme assuming constant accelerations between each update interval Δt according to

$$\begin{aligned} v_\alpha(t + \Delta t) &= v_\alpha(t) + a_\alpha(t)\Delta t, \\ x_\alpha(t + \Delta t) &= x_\alpha(t) + v_\alpha(t)\Delta t + \frac{1}{2}a_\alpha(t)(\Delta t)^2. \end{aligned} \tag{21}$$

3.1 String stability of a platoon

We have investigated the stability of the HDM as a function of the reaction time T' and the number n_a of anticipated vehicles by simulating a platoon of 100 vehicles following an externally controlled lead vehicle. As in a similar study for the OVM [12,9], the lead vehicle drives at $v_{\text{lead}} = 15.34$ m/s for the first 1000 s before it decelerates with -0.7 m/s² to 14.0 m/s and continues with this velocity until the simulation ends at 2500 s.

For the platoon vehicles, we set the IDM parameters $v_0 = 32$ m/s and $T = 1.5$ s to obtain the same desired velocity and initial equilibrium distance ($s_e = 25.7$ m) as in previous studies [12,9]. The other IDM parameters are those of Table 1. If n_a is larger than the number of preceding vehicles (which can happen for the first vehicles of the platoon) then n_a is reduced accordingly. Neither fluctuations nor memory effects have been activated in this scenario. As initial conditions, we assumed the platoon to be in equilibrium.

We distinguish three stability regimes. (i) String stability, i.e., all perturbations introduced by the deceleration of the lead vehicles are damped away, (ii) an oscillatory regime, where perturbations increase but do not lead to crashes, (iii) an instability with accidents. Oscillating behavior was detected if the maximum deceleration of all vehicles in all time steps exceeded 2 m/s². Figure 1 shows the three phases depending on the reaction time T' and on the platoon size for a spatial anticipations of $n_a = 1$ and 5 vehicles, respectively.

For $n_a = 1$ (corresponding to conventional car-following models without spatial anticipation), a platoon of 100 vehicles is stable for reaction times of up to $T'_{c1} = 0.8$ s. Test runs with larger platoon sizes (up to 1000 vehicles) did not result in different thresholds suggesting that stability for a platoon size of 100 essentially means stability for arbitrarily large platoon sizes.

Increasing the spatial anticipation to $n_a = 5$ vehicles shifted the threshold of the delay time T' for string stability of a platoon of 100 vehicles to $T'_{c1} = 1.3$ s. Increasing the delay time T' beyond the stability threshold lead to strong oscillations of the platoon. Crashes, however, occurred only when T' exceeded a second threshold T'_{c2} . Remarkably, for $n_a = 5$ or more vehicles, the observed threshold $T'_{c2} = 1.8$ s is larger than the equilibrium time headway $s_e/v_{\text{lead}} = 1.68$ s. More detailed investigations revealed that crashes were triggered either directly by late reactions to deceleration maneuvers or indirectly as a consequence of the string instability. Further increasing n_a did not change the thresholds significantly.

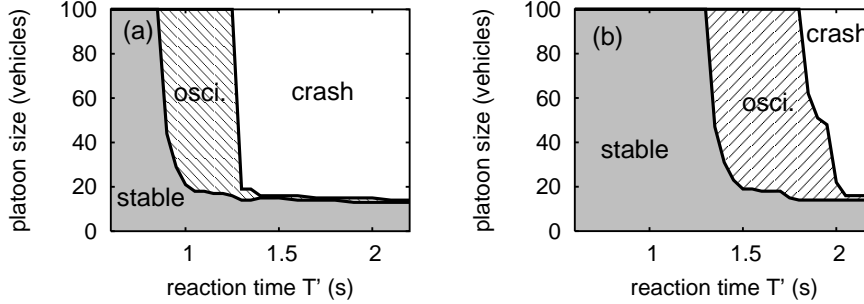


Fig. 1. Stability of a platoon of identical vehicles as a function of the platoon size and the reaction time T' for the situation described in Section 3.1 (a) for follow-the-leader behavior ($n_a = 1$), and (b) for a reaction to $n_a = 5$ vehicles. The simulation is for a time headway of $T = 1.5$ s, a numerical update time interval of $\Delta t = 0.1$ s, and a desired velocity $v_0 = 32$ m/s. The other parameters are those specified in Table 2. In the 'stable' phase, all perturbations are damped away. In the oscillatory regime, the perturbations increase, but do not lead to crashes.

3.1.1 Relation between reaction time and numerical update time interval

We have systematically investigated the effects of various combinations of T' and Δt for a platoon size of 100 vehicles. Figure 2 shows our results in form of a phase diagram spanned by both times. Interestingly, for equal numerical values of T' and Δt , the combination $(T', \Delta t \approx 0)$ leads to stronger destabilizing effect than the combination $(0, \Delta t)$. Notice that multi-anticipation allows for stable traffic at update time intervals exceeding 2 s, i.e. nearly twice the time headway.

To explain this finding, it is essential, to distinguish between the reaction time T' and Δt . To illustrate the difference, let us consider (i) the limiting case $\Delta t \rightarrow 0$ with $T' = T_0 > 0 = \text{const.}$ (exact solution of the time-continuous model for a finite reaction time, horizontal axis of Fig. 2), (ii) the case $\Delta t = T_0$ and $T' = 0$ (numerical solution according to (21) for zero reaction time, vertical axis of Fig. 2). In case (i), the acceleration at any time t is calculated using the information available at $t - T_0$. For the complementary case (ii), the acceleration is calculated at the beginning of each time step using the actual information, but it is not updated during each time step. This means, the *effective* reaction time for case (ii) varies between 0 and T_0 at the beginning and end of each time step, respectively. Consequently, a reaction time $T' = T_0$ has a stronger destabilizing effect than an update time interval of the same numerical value. This is consistent with the results of Fig. 2. Remarkably, for $n_a = 1$ (part (a) of this figure), the borderline between stable and oscillatory platoons is given by $\Delta t + 2T' = 1.7$ s. For $n_a = 5$ (part (b)), this borderline is given by $\Delta t + 2T' \approx 2.8$ s provided $\Delta t \leq 2$ s. This means, the destabilizing effect of a finite reaction time is about twice that of a finite update time interval of the same numerical value or, *cum grano salis*, the *effective* reaction time introduced by a finite update time interval is about $T'_{\text{eff}} = \Delta t/2$.

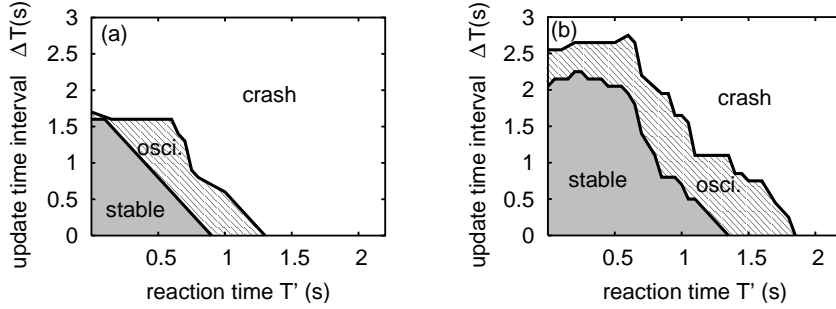


Fig. 2. The three dynamical phases for a platoon size of 100 vehicles as a function of reaction time and numerical time discretization (a) for follow-the-leader behavior ($n_a = 1$) and (b) for a reaction to $n_a = 5$ preceding vehicles.

Notice that, besides the numerical necessity for a finite Δt , the value of Δt can be interpreted as a typical length of time periods where drivers do not draw their attention to the driving task. In contrast to the event-driven approach in [27], however, drivers revert their attention to traffic on a time-oriented basis.

3.2 Open system with a bottleneck

In this section we examine the compensating influences of driver reaction times T' and spatial anticipation n_a on the stability of traffic and the occurring traffic states in a more complex and realistic situation.

We have simulated a single-lane road section of total length 20 km with a bottleneck and open boundaries. Moreover, we have assumed identical drivers and vehicles of length $l = 5$ m whose HDM parameters are given by Table 2. The update time interval of the numerical integration was $\Delta t = 0.2$ s. Each simulation run covered a time interval of 3 h. We initialized the simulations with very light traffic (traffic density 1 vehicle/km) and set all initial velocities to 100 km/h. Notice that the initial conditions are relevant only for the time interval needed by the vehicles to cross the road section, i.e., for about the first 15 min.

We simulated idealized rush-hour conditions by increasing the inflow $Q_{in}(t)$ at the upstream boundary linearly from 100 veh/h at $t = 0$ to 2100 veh/h at $t = 1$ h and keeping the traffic demand constant at $Q_{in} = 2100$ veh/h afterwards. Since this demand exceeds the static road capacity $Q_{max} \approx 2000$ veh/h at the bottleneck (the maximum of the fundamental diagram), a traffic breakdown is always provoked, even for values of T' and n_a corresponding to stable traffic. Both the initial vehicles and the vehicles of the inflow have been initialized with a 'memory' of free traffic, cf. [21].

We have implemented a flow-conserving bottleneck at $18 \text{ km} \leq x \leq 20 \text{ km}$

by linearly increasing the IDM parameter T from 1.1 s to 1.65 s in the region $18.0 \text{ km} \leq x \leq 18.5 \text{ km}$, setting $T = 1.65 \text{ s}$ for $18.5 \text{ km} \leq x \leq 19.5 \text{ km}$, and linearly decreasing T from 1.65 s to 1.1 s in the region $19.5 \text{ km} \leq x \leq 20.0 \text{ km}$.

In order to determine the spatiotemporal dynamics, we plot, at any given spatiotemporal point (x, t) , the locally averaged velocity of the vehicle trajectories nearby. The averaging filter had half-widths of 1 minute and 0.4 kilometers, respectively.

3.2.1 Phase diagram

We have performed simulation runs with various combinations of the number of anticipated vehicles ($n_a = 1, \dots, 8$) and reaction times ($T' = 0, \dots, 1.6 \text{ s}$). Figure 3 shows the resulting dynamic traffic regimes in the space spanned by n_a and T' . The other parameters given in Table 1 and 2 are kept constant. The results are robust against variations of these parameters.

The left lower corner corresponds to the special case of the IDM with memory (IDMM), i.e. to the case of zero reaction time and taking into account only the immediate front vehicle. In this case, the simulation leads to oscillatory congested traffic (OCT), cf. Figures 4(a), 6(a), and 7(a). In the OCT state, congested traffic is linearly unstable and small perturbations grow while travelling backwards [41,4].

Varying n_a and T' leads to following main results: (i) Traffic stability increases drastically when increasing the spatial anticipation from $n_a = 1$ to 5, while the stability remains essentially unchanged when increasing n_a further to values > 5 . In particular, for a sufficiently large number of anticipated vehicles, the congestion becomes stable (HCT, homogeneous congested traffic) as shown in Fig. 4(b). Thus, different traffic states can be produced not only by varying the bottleneck strength as in the phase diagram proposed in Ref. [41], but also by varying model parameters that influence stability. (ii) Increasing the reaction time T' destabilizes traffic and finally leads to crashes. For a given n_a , the critical threshold T'_{c2} for crashes is somewhat lower than in the simulations of Sec. 3.1, which is caused by the more complex scenario and by the higher braking decelerations caused by the traffic breakdown. (iii) The other dynamic congested traffic states of the phase diagram of Ref. [41] are found as well, specifically, triggered stop-and-go waves (TSG), cf. Figures 4(c) and (e), plus an interesting combination of moving localized clusters (MLC) and pinned localized clusters (PLC), cf. Fig. 4(d).

Remarkably, the destabilizing effects of finite reaction times can be compensated to a large extent by the spatial and temporal anticipation of the HDM such that the resulting stability and dynamics are similar to the IDM(M)

case of zero anticipation and reaction time. This is illustrated by comparing Fig. 4(a) (no reaction time and no anticipation) with Fig. 4(e) (finite reaction time and anticipation). Notice, however, that the wavelengths of the stop-and-go waves in Fig. 4(e) are larger and the transitions between 'stop' and 'go' smoother than those of Fig. 4(a). It turns out that the time scales of the simulation with multi-anticipation, Fig. 4(e), agrees well with real traffic data [42]. Obviously, multi-anticipation plays an important role for the collective dynamics in real traffic. Interestingly, the effects on the car-following dynamics itself is less pronounced. For example, the simulated velocity-velocity correlations turned out to be very short-ranged, in agreement with observations based on single-vehicle data [15].

Figure 4(c) shows a complex traffic state with nearly homogeneous congested traffic near the bottleneck and stop-and-go waves further upstream. This can be understood by distinguishing between linear and convective stability. Near the bottleneck, the congested traffic is linearly unstable, i.e., small perturbations created by the fluctuating terms of the model will grow. However, while growing, the perturbations travel upstream and will eventually be carried out of the system leaving homogeneous congested traffic behind as soon as the fluctuations are negligible. This means, the congested region near the bottleneck is convectively stable. Thus, the sometimes observed complex transition from free traffic *via* homogeneous congested traffic ('synchronized traffic') to stop-and-go traffic can possibly be explained by fluctuating terms in the acceleration connected with a congested region near the bottleneck that is simultaneously linearly unstable but convectively stable.

We have compared the spatiotemporal dynamics with traffic data from the German freeway A9 South near Munich. For this freeway, aggregated detector data (vehicle counts and average velocities for one-minute intervals) are available for each lane at the locations indicated in Fig. 5 (a).

The plots (b) and (c) of Figure 5 show the spatiotemporal dynamics of the local velocity for triggered stop-and-go traffic (TSG) and oscillating congested traffic (OCT), respectively. In both cases, these states were caused by intersections acting as bottlenecks.

To obtain the spatiotemporal dynamics shown in these plots, we have applied the adaptive smoothing method (ASM) [43] to the lane-averages of the velocity data. The smoothing times and lengths of the ASM are set to the values used for the averaging filter in the simulation, i.e., to 1 min and 0.4 km, respectively. The other ASM parameters were set to $v_{c1} = 30$ km/h, $v_{c2} = 60$ km/h, $c_{\text{free}} = 80$ km/h, and $c_{\text{cong}} = -15$ km/h [43]. We have checked that the result was essentially unchanged when changing any of the first three parameters by factors between 0.7 and 1.5. In contrast, changes of the last parameter c_{cong} representing the propagation velocity of collective structures in congested

traffic influence the result. Artificial shifts of the congested structures are observed if c_{cong} is outside a range of about $[-17 \text{ km/h}, -14 \text{ km/h}]$. This means, besides making spatiotemporal plots, the ASM can be used to determine the propagation velocity c_{cong} as well.

By comparing the simulation results 4(a) and (e) with the traffic data shown in 5(b) and (c), one sees a qualitative agreement of the spatiotemporal dynamics in many respects. Particularly, (i) the congestion is triggered by a bottleneck, (ii) the downstream front of the congestion is stationary and located at the position of the bottleneck, (iii) traffic is essentially non-oscillatory in a region of about 1 km width near the bottleneck (this is sometimes called the 'pinch region' [44]), (iv) further upstream, the congested traffic consists of 'stop-and-go' waves propagating upstream at a constant velocity c_{cong} , (v) the period τ of the oscillations is variable with typical values between 5 and 30 minutes where smaller periods typically correspond to more severe congestions.

The isolated moving localized cluster (MLC) in the simulation of Fig. 4(a), which was triggered approximately at time $t = 1 \text{ h}$ is not seen in the data. However, such combined states and all the other states shown in Fig. 4 are observed in traffic data as well [42]. Particularly, PLC and MLC states occurred in Fig. 6 and Fig. 10 of Ref. [42]. HCT states and even combined states of one or more PLCs with one or more isolated MLCs were observed in [42] as well.

In addition to these qualitative aspects, there exists a nearly quantitative agreement with respect to (i) the propagation velocity $c_{\text{cong}} = -15 \text{ km/h}$, and (ii) the range of the oscillation periods of $5 \text{ min} \leq \tau \leq 40 \text{ min}$ (notice that many car-following models yield too short periods).

In summary, the traffic states of Fig. 4 are qualitatively identical to those found for the macroscopic gas-kinetic-based traffic model (GKT)[41,50] and the microscopic IDM [29]. Notice, however, that the approach to obtaining congested traffic states in the previous publications is conceptually different from that of the present work. In Refs. [41,50,29] we varied external control parameters such as traffic flows and bottleneck strengths to obtain an '*extrinsic*' phase diagram. In the present work, we kept external parameters constant and varied model parameters influencing the stability to obtain an '*intrinsic*' diagram. The analytic expressions for approximate phase boundaries presented in [41,29] apply to both, external quantities such as traffic flow and intrinsic quantities such as stability limits. Hence, they remain valid.

3.2.2 Virtual detector data

Figure 6 shows flow-density data of a virtual detector at position $x = 14 \text{ km}$ (5 km upstream of the bottleneck) with a sampling period of 1 min. In agreement with real traffic data [45], the data cover a two-dimensional area in

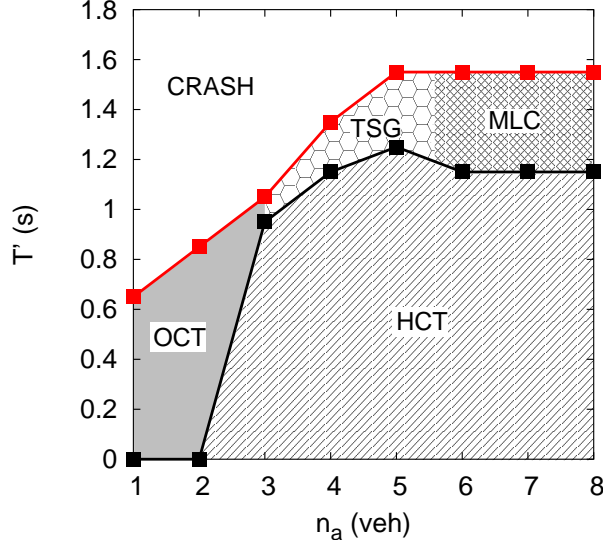


Fig. 3. Phase diagram of congested traffic states in the space spanned by the number n_a of anticipated vehicles and the reaction time T' in the open system with a bottleneck described in the text. For all simulations, the traffic demand $Q_{in}(t)$ was linearly increased from $Q_{in}(t) = 100$ veh/h to 2100 veh/h in the first hour and kept constant afterwards. Homogeneous congested traffic (HCT) corresponds to a congested regime which is stable with respect to perturbations. The other states OCT (oscillatory congested traffic), TSG (triggered stop-and-go traffic), and MLC (moving localized cluster) are discussed in the main text.

the congested region, both for the IDMM [Fig. 6(a)] and for the HDM with finite reaction times and anticipations [Fig. 6(b)].

Since the HDM has a unique equilibrium flow-density curve and we have simulated identical driver-vehicle combinations, the observed scattering implies that the simulated congested traffic is out of equilibrium. In the simulations, possible forces bringing traffic out of equilibrium are (i) the fluctuating terms of the HDM, (ii) traffic instabilities. The distance from the equilibrium curve (and thus the area of scattering) is increased by the long relaxation times back to equilibrium implied by the adaptation of the driver behavior to the traffic environment (memory effect). It turns out that traffic instabilities contribute much more to the scattering of the flow-density data than the fluctuating terms. Notice, however, that in real traffic the heterogeneity of the driving styles and vehicle types plays an important role as well [34,46,47,22], which is discussed in more detail in [21]. Figure 7 shows velocity time series of the same virtual detectors. Compared to the IDMM, the finite reaction times and anticipations of the HDM lead to a larger period of velocity oscillations (about 10 min for the HDM compared to 6 min for the IDMM) and to softer upstream congestion fronts, i.e., to lower velocity gradients. Remarkably, the periods and gradients of the velocity time series of the HDM agree well with those of real OCT data, cf, e.g., Fig. 12 in Ref. [29].

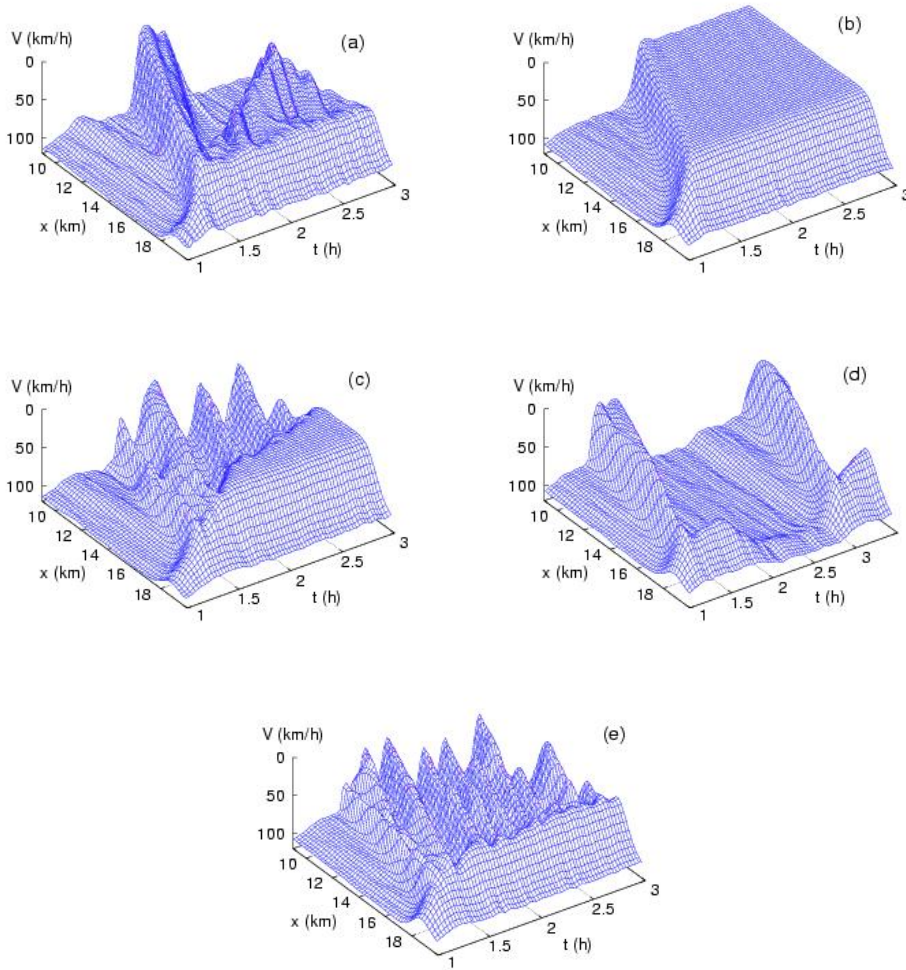


Fig. 4. Spatiotemporal dynamics of typical traffic states occurring in the phase diagram of Fig. 3. (a) $n_a = 1$, $T' = 0$ s (special case of the IDMM [21]) leading to OCT; (b) $n_a = 5$, $T' = 0.5$ s (HCT); (c) $n_a = 5$, $T' = 1.2$ s (TSG); (d) $n_a = 8$, $T' = 1.2$ s (MLC and PLC); (e) $n_a = 5$, $T' = 1.25$ s (TSG). All data are smoothed with half-widths of 1 min and 0.4 km, respectively.

3.2.3 Dynamic capacity: Outflow from congested traffic

We have measured the averaged outflow Q_{out} from congested traffic at the downstream front located near the bottleneck using a virtual detector immediately downstream of the front at $x = 18750$ m. Q_{out} can be considered as a dynamical road capacity [48]. To average over the oscillations of OCT states, we have used an increased sampling time interval of $T_{\text{aggr}} = 30$ min.

Figure 8 shows Q_{out} as a function of the number of anticipated vehicles for two values $T' = 0.6$ s and $T' = 1.0$ s of the reaction time. Increasing the number of anticipated vehicles from $n_a = 1$ to $n_a = 5$ leads to an increase of the dynamical road capacity by about 15%. A further increase of n_a yielded no

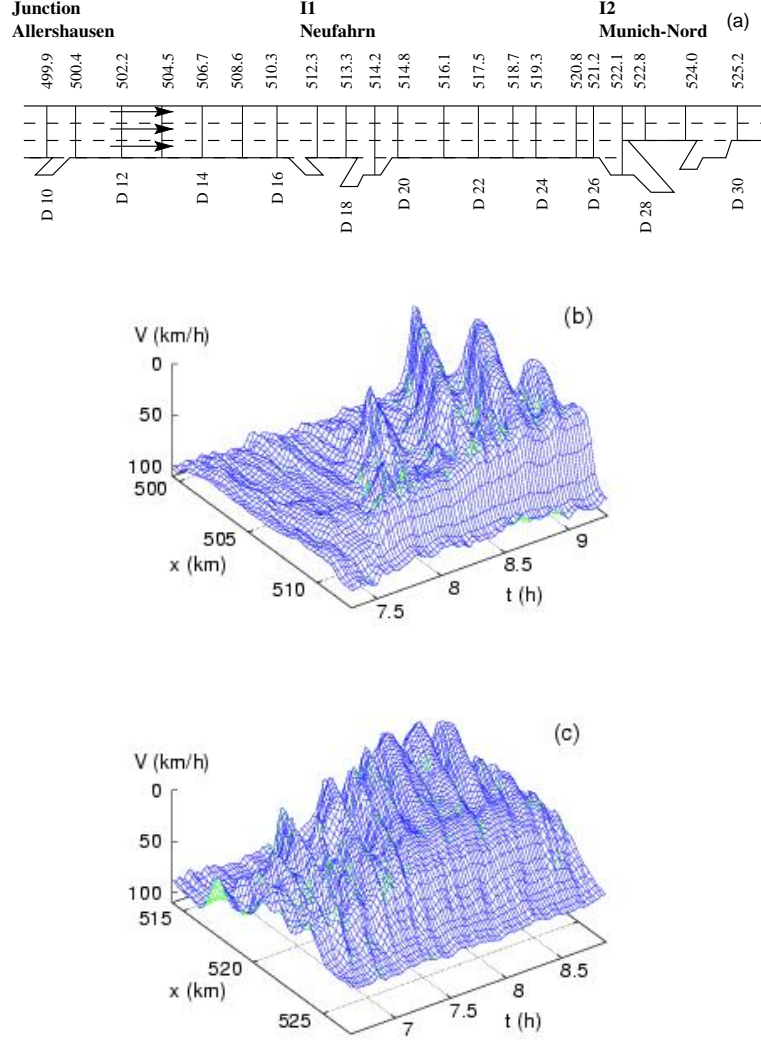


Fig. 5. Spatiotemporal dynamics of congested traffic on the German freeway A9 South near Munich. (a) Sketch of the freeway; (b) Triggered stop-and-go traffic (TSG) triggered by the intersection II; (c) Oscillatory congested traffic (OCT) state caused by the intersection I2. The spatiotemporal data were obtained from one minute data at the detector positions indicated in (a) using the adaptive smoothing method with smoothing half-widths of 1 min and 0.4 km, respectively.

significant changes. Remarkably, up to $T' = 1.2$ s, the dynamic capacity Q_{out} depends only marginally on the reaction time.

4 Discussion

Finite reaction times, limited attention spans, and errors in estimating the input variables are clearly essential factors affecting performance and stability

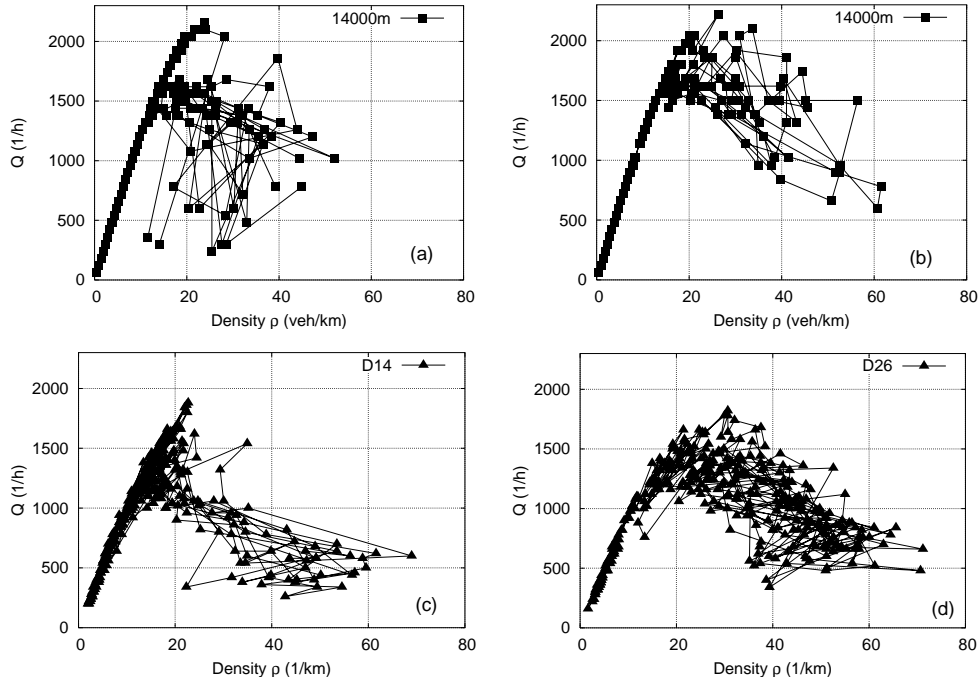


Fig. 6. Simulated flow-density data at $x = 14.0$ km measured by a virtual detector with sampling interval $T_{aggr} = 60$ s. (a) Special case of the IDMM ($n_a = 1$, $T' = 0$ s) leading to OCT, (b) finite anticipation and reaction time ($n_a = 5$, $T' = 1.2$ s) leading to TSG, (c),(d) real traffic data from the German freeway A9 South, cf. Fig. 5(a).

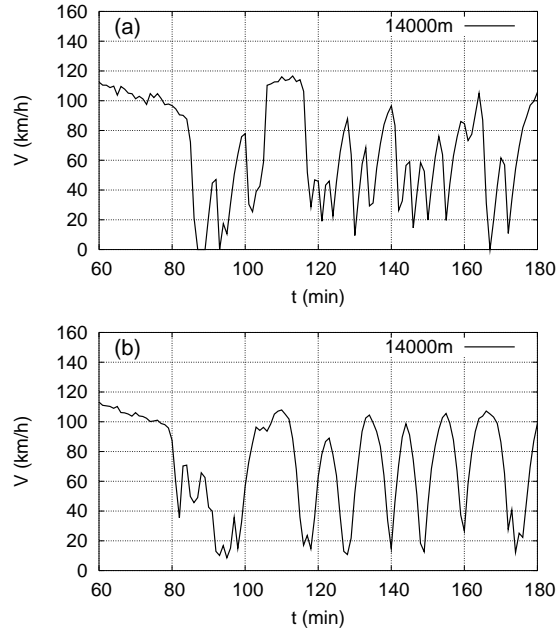


Fig. 7. Velocity time series by a virtual detector at $x = 14$ km for (a) $n_a = 1$, $T' = 0$ s, and (b) $n_a = 5$, $T' = 1.2$ s. Notice the increase of the oscillation wavelength in the scenario (b) with anticipation.

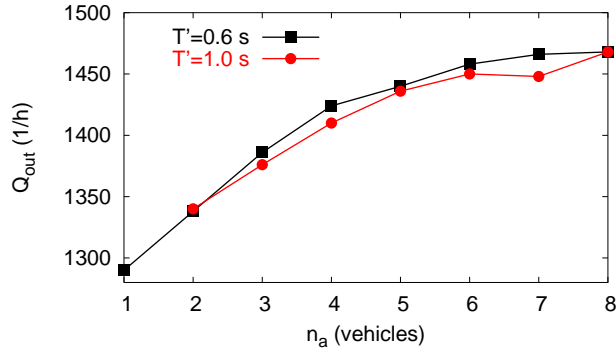


Fig. 8. Average outflow from the stationary downstream front of congested traffic located at the bottleneck for $T' = 1.0$ and 0.6 s.

of vehicular traffic. This applies not only to human drivers but (to a lesser extent) also to realistic, i.e., imperfect, automated driving-assistance systems. Human drivers, on the other hand, may offset these destabilizing effects by looking several vehicles ahead, anticipating the future traffic situation, and adapting to the traffic environment.

In contrast, these aspects are rarely considered in traffic modelling. Common continuous microscopic models such as the optimal-velocity model [11] or the IDM neglect them all, and also recent advances such as the boundedly rational driver model [30,31] or generalizations of the optimal-velocity model [9] implement only one or two of them. Nevertheless, the simple models allow to describe many, particularly macroscopic, aspects of traffic dynamics such as the spatiotemporal dynamics of the various types of traffic congestions, the propagation of stop-and-go traffic, or even the scattering of flow-density data points of 'synchronized traffic'.

The question arises why, despite their obvious shortcomings, the simple models work so well. This question became more pressing after it turned out that all of the above models (including the IDM) produce unrealistic dynamics and even crashes when realistic reaction times (of the order of 1 s) are simulated but the models are left unchanged, otherwise [8,12]. This clearly shows that, e.g., reaction times are crucial and that the simple models neglect essential elements of the human driving strategy.

In this work, we showed that the destabilizing effects of reaction times and estimation errors can be counterbalanced by spatial and temporal anticipations explaining the good performance of the simple models. We provided quantitative detail for this offset and for the remaining differences in the dynamics which can be applied to formulate application criteria and limits for using the simple models. It should be mentioned that anticipation plays a stabilizing role in other multi-agent systems as well, such as in supply chains [49].

The main contribution of this work is a general scheme to include all of the

above effects to a wide class of car-following models. As main result, we have found that, when applied to the IDM, reaction times and estimating uncertainties can essentially be compensated by spatial and temporal anticipation, i.e., one obtains essentially the same longitudinal dynamics. This means, when applying the HDM to a basic model, one tends to obtain essentially the same longitudinal dynamics as with the basic model (in our case, the IDM) itself. Since the basic models have both the advantages and limitations of adaptive cruise control (ACC) systems, one can investigate the impact of ACC vehicles on the capacity and stability of the overall traffic simply by simulating a mixture of, e.g., IDM and HDM vehicles. Furthermore, one gets the nontrivial result that hypothetical future traffic consisting predominantly of automated vehicles will exhibit macroscopic dynamics similar to that of the actual traffic, although the driving strategy would be markedly different.

While finite reaction times has been investigated as early as 1961 [7], the HDM-IDM combination is, to our knowledge, the first model allowing accident-free driving at realistic accelerations in all traffic situations for reaction times of the order of and even exceeding the time headway. It is straightforward to use any other micromodel where the acceleration depends only on positions, velocities and accelerations of the own and the preceding vehicle such as the optimal-velocity model [11], the Gipps model [28], or the boundedly rational driver model [30,31].

A comparison of the stochastic HDM expressions for imperfect estimating capabilities with other stochastic micromodels is in order. While fluctuating terms were introduced to traffic models more than 20 years ago [25], the most prominent example of stochastic traffic models are cellular automata (CA) of the Nagel-Schreckenberg type [10] and extensions thereof. There is, however, a qualitative difference compared to most continuous models: Fluctuating terms change the qualitative dynamics of many CA models and typically are required to yield plausible results. In contrast, the qualitative dynamics of many time-continuous micromodels such as the OVM or the IDM is not altered qualitatively by not too large fluctuations.

A closer look at quantitative features of stop-and-go traffic or oscillations, as recorded by virtual detectors, shows that the dynamics of the HDM agrees better with actual traffic data than that produced by the simple models mentioned above. In the latter, the gradients typically are too large and the periods between two 'stop' waves too short. Thus it seems that the large discrepancy between the 'microscopic' time scales for adapting distances and velocities (of the order of 10 s) and the observed macroscopic time scales (of the order of 10 min or more for the period between two 'stop' waves) are caused, at least partly, by multi-anticipation of human drivers.

The phase diagram, Fig. 3, contains qualitatively the same spatiotemporal

congested states as found in Refs. [41,29]. At first sight, this seems surprising since, besides using a different model, the control parameters making up the phase space were extrinsic in the previous publications while the phase space is spanned by intrinsic model parameters in the present work. A closer look at the analytic expressions for the phase boundaries [41] containing both extrinsic flow parameters and intrinsic stability limits shows that variations of both kinds of control parameters can lead to phase transitions.

In addition to the congested states of Ref. [41], the HDM includes complex traffic breakdown scenarios such as the coexistence of free traffic, homogeneous congested traffic, and triggered stop-and-go waves. Such states, called 'generalized patterns' in the nomenclature of Kerner, have been observed on some German freeways [45,42], see also Fig. 5(b). Simulations with the HDM suggest as general mechanism for such states, namely an interplay between the fluctuations induced by estimation errors and the macroscopic dynamics in the homogeneously congested region which must be convectively stable but linearly unstable.

From a control-theoretical point of view, the HDM, in the limit of negligible update time intervals, implements a continuous response to delayed and noisy input stimuli. Alternatively, human driving behavior has been modelled by so-called action-point models, where the response changes discontinuously whenever certain boundaries in the space spanned by the input stimuli are crossed [51,52,27,18], but these thresholds could not be empirically confirmed. It has been proposed that distractions and the 'restricted attention span' of human drivers play an important role in driving behavior as well [53]. In the HDM, a restricted attention can be modelled simply by increasing the update time interval of the explicit numerical scheme to values up to 2.5 s (cf. Fig. 2) and identifying the update interval as the typical time interval where the attention of the driver is not focussed on traffic. Since the reaction time can be varied independently from the update interval, the combined effects of distractions and finite reaction times can be investigated simultaneously.

In modelling the estimation errors we included the persistency of estimation errors for a certain time interval by a stochastic Wiener process whose distinct feature is a finite correlation time. It turned out that Wiener processes are a very efficient tool to incorporate persistent perception errors into time-continuous models. Another example of such errors would be the uncertainties in estimating the fundamental price of assets in a stock market.

Finally, it should be mentioned that, in this work, we have considered only longitudinal aspects (acceleration and deceleration) of human driving and implemented only identical driver-vehicle units. Platooning effects due to different driving styles and the remarkable ability of human drivers to safely and smoothly change lanes even in congested conditions are the topic of a

forthcoming paper.

Acknowledgments: The authors would like to thank for partial support by the DFG project He 2789/2-2 and the Volkswagen AG within the BMBF project INVENT.

References

- [1] M. Brackstone, M. McDonald, Car-following: a historical review, *Transp. Res. F* 2 (1999) 181–196.
- [2] E. Holland, A generalised stability criterion for motorway traffic, *Transp. Res. B* 32 (1998) 141–154.
- [3] D. Helbing, Traffic and related self-driven many-particle systems, *Review of Modern Physics* 73 (2001) 1067–1141.
- [4] D. Helbing, M. Treiber, Critical discussion of "synchronized flow", *Cooperative Transportation Dynamics* 1 (2002) 2.1–2.24, (*Internet Journal*, www.TrafficForum.org/journal).
- [5] M. Treiber, D. Helbing, Microsimulations of freeway traffic including control measures, *Automatisierungstechnik* 49 (2001) 478–484.
- [6] G. Marsden, M. McDonald, M. Brackstone, Towards an understanding of adaptive cruise control, *Transportation Research C* 9 (2001) 33–51.
- [7] G. Newell, Nonlinear effects in the dynamics of car following, *Operations Research* 9 (1961) 209.
- [8] M. Bando, K. Hasebe, K. Nakanishi, A. Nakayama, Analysis of optimal velocity model with explicit delay, *Phys. Rev. E* 58 (1998) 5429.
- [9] L. Davis, Modifications of the optimal velocity traffic model to include delay due to driver reaction time, *Physica A* 319 (2002) 557.
- [10] K. Nagel, M. Schreckenberg, A cellular automaton model for freeway traffic, *J. Phys. I France* 2 (1992) 2221–2229.
- [11] M. Bando, K. Hasebe, A. Nakayama, A. Shibata, Y. Sugiyama, Dynamical model of traffic congestion and numerical simulation, *Phys. Rev. E* 51 (1995) 1035–1042.
- [12] L. Davis, Comment on 'analysis of optimal velocity model with explicit delay', *Phys. Rev. E* 66 (2002) 038101.
- [13] W. Knospe, L. Santen, A. Schadschneider, M. Schreckenberg, Human behaviour as origin of traffic phases, *Phys. Rev. E* 65 (2001) 015101.

- [14] B. Tilch, D. Helbing, Evaluation of single vehicle data in dependence of the vehicle-type, lane, and site, in: D. Helbing, H. Herrmann, M. Schreckenberg, D. Wolf (Eds.), *Traffic and Granular Flow '99*, Springer, Berlin, 2000, pp. 333–338.
- [15] W. Knospe, L. Santen, A. Schadschneider, M. Schreckenberg, Single-vehicle data of highway traffic: Microscopic description of traffic phases, *Phys. Rev. E* 65 (2002) 056133.
- [16] M. Green, "How Long Does It Take to Stop?" methodological analysis of driver perception-brake times, *Transportation Human Factors* 2 (2000) 195–216.
- [17] H. Lenz, C. Wagner, R. Sollacher, Multi-anticipative car-following model, *European Physical Journal B* 7 (1998) 331–335.
- [18] N. Eissfeldt, P. Wagner, Effects of anticipatory driving in a traffic flow model, *European Physical Journal B* 33 (2003) 121–129.
- [19] H. K. Lee, R. Barlovic, M. Schreckenberg, D. Kim, Mechanical restriction versus human overreaction triggering congested traffic states, *Physical Review Letters* 92 (2004) 238702.
- [20] W. Brilon, M. Ponzlet, Application of traffic flow models, in: D. E. Wolf, M. Schreckenberg, A. Bachem (Eds.), *Traffic and Granular Flow*, World Scientific, Singapore, 1996, pp. 23–40.
- [21] M. Treiber, D. Helbing, Memory effects in microscopic traffic models and wide scattering in flow-density data, *Phys. Rev. E* 68 (2003) 046119.
- [22] K. Nishinari, M. Treiber, D. Helbing, Interpreting the wide scattering of synchronized traffic data by time gap statistics, *Phys. Rev. E* 68 (2003) 067101.
- [23] M. Treiber and D. Helbing, *Explanation of observed features of self-organization in traffic flow*, e-print cond-mat/9901239.
- [24] D. Helbing, I. J. Farkas, D. Fasold, M. Treiber, T. Vicsek, Critical discussion of "synchronized flow" simulation of pedestrian evacuation, and optimization of production processes, in: *Traffic and Granular Flow 2001*, Springer, Berlin, 2002, pp. 511–530.
- [25] P. G. Gipps, A behavioural car-following model for computer simulation, *Transp. Res. B* 15 (1981) 105–111.
- [26] P. Hidas, Modelling lane changing and merging in microscopic traffic simulation, *Transportation Research C* 10 (2002) 351–371.
- [27] P. Wagner, I. Lubashevsky, Empirical basis for car-following theory development, cond-mat/0311192.
- [28] P. G. Gipps, A model for the structure of lane-changing decisions, *Transp. Res. B* 20B (1986) 403–414.

- [29] M. Treiber, A. Hennecke, D. Helbing, Congested traffic states in empirical observations and microscopic simulations, *Physical Review E* 62 (2000) 1805–1824.
- [30] I. Lubashevsky, P. Wagner, R. Mahnke, Bounded rational driver models, *European Physical Journal B* 32 (2003) 243.
- [31] I. Lubashevsky, P. Wagner, R. Mahnke, Rational-driver approximation in car-following theory, *Phys. Rev. E* 68 (2003) 056109.
- [32] E. Brockfeld, R. Kühne, P. Wagner, Towards benchmarking microscopic traffic flow models, in: W. Möhlenbrink, M. Bargende, U. Hangleiter, U. Martin (Eds.), *Networks for Mobility 2002, FOVUS: International Symposium*, September 18–20, Stuttgart, Stuttgart, 2002, pp. 321–331.
- [33] L. Edie, R. Foote, Traffic flow in tunnels, in: H. Orland (Ed.), *Highway Research Board Proceedings, 37th annual meeting*, National Academy of Sciences, Washington D.C., 1958.
- [34] M. Treiber, A. Hennecke, D. Helbing, Microscopic simulation of congested traffic, in: D. Helbing, H. Herrmann, M. Schreckenberg, D. Wolf (Eds.), *Traffic and Granular Flow '99*, Springer, Berlin, 2000, pp. 365–376.
- [35] Inclusion of the acceleration $a_{\alpha-1}(t)$ of the preceding vehicle to the input variables is straightforward allowing for micromodels that model reactions to braking lights.
- [36] Generally, the estimation error concludes a systematic bias as well. We found that our model is very robust with respect to reasonable biases in distance and velocity-difference estimates.
- [37] C. Gardiner, *Handbook of Stochastic Methods*, Springer, N.Y., 1990.
- [38] W. Knospe, L. Santen, A. Schandschneider, M. Schreckenberg, Disorder effects in cellular automata for two-lane traffic, *Physica A* 265 (1998) 614–633.
- [39] M. Treiber, D. Helbing, Realistische Mikrosimulation von Strassenverkehr mit einem einfachen Modell, in: D. Tavangarian, R. Grützner (Eds.), *ASIM 2002, Tagungsband 16. Symposium Simulationstechnik*, Rostock, 2002, pp. 514–520.
- [40] M. Fukui, Y. Sugiyama, M. Schreckenberg, D. E. W. (eds.), *Traffic and Granular Flow '01*, Springer, Berlin, 2003.
- [41] D. Helbing, A. Hennecke, M. Treiber, Phase diagram of traffic states in the presence of inhomogeneities, *Phys. Rev. Lett.* 82 (1999) 4360–4363.
- [42] M. Schönhof, D. Helbing, Empirical Features of Congested Traffic States and their Implications for Traffic Modeling, *cond-mat/0408138*.
- [43] M. Treiber, D. Helbing, Reconstructing the spatio-temporal traffic dynamics from stationary detector data, *Cooper@tive Tr@nsport@tion Dyn@mics 1* (2002) 3.1–3.24, (*Internet Journal, www.TrafficForum.org/journal*).

- [44] B. Kerner, Experimental features of self-organization in traffic flow, *Phys. Rev. Lett.* 81 (1998) 3797–3800.
- [45] B. Kerner, Empirical macroscopic features of spatio-temporal traffic patterns at highway bottlenecks, *Phys. Rev. E* 65 (2002) 046138.
- [46] J. H. Banks, An investigation of some characteristics of congested flow (1999).
- [47] M. Treiber, D. Helbing, Macroscopic simulation of widely scattered synchronized traffic states, *J. Phys. A* 32 (1) (1999) L17–L23.
- [48] F. Hall, K. Agyemang-Duah, Freeway capacity drop and the definition of capacity, *Transportation Research Record* 1320 (1991) 91–108.
- [49] T. Nagatani, D. Helbing, Stability analysis and stabilization strategies for linear supply chains, *Physica A* 335 (2004) 644.
- [50] M. Treiber, A. Hennecke, D. Helbing, Derivation, properties, and simulation of a gas-kinetic-based, non-local traffic model, *Phys. Rev. E* 59 (1999) 239–253.
- [51] E. P. Todosiev, The action-point model of the driver-vehicle system, Technical report 202a-3, Ohio State University, Columbus, Ohio (1963).
- [52] R. Wiedemann, *Simulation des Straßenverkehrsflusses*, Schriftenreihe des IfV Vol. 8, Institut für Verkehrswesen, Universität Karlsruhe (1974).
- [53] E. Boer, Car following from the driver’s perspective, *Transp. Res. F* 2 (1999) 201–206.